

Monitoring the frozen duration of Qinghai Lake using satellite passive microwave remote sensing low frequency data

CHE Tao[†], LI Xin & JIN Rui

Cold and Arid Regions Environment and Engineering Research Institute, Chinese Academy of Sciences, Lanzhou 710000, China

The Qinghai Lake is the largest inland lake in China. The significant difference of dielectric properties between water and ice suggests that a simple method of monitoring the Qinghai lake freeze-up and break-up dates using satellite passive microwave remote sensing data could be used. The freeze-up and break-up dates from the Qinghai Lake hydrological station and the MODIS L1B reflectance data were used to validate the passive microwave remote sensing results. The validation shows that passive microwave remote sensing data can accurately monitor the lake ice. Some uncertainty comes mainly from the revisit frequency of satellite overpass. The data from 1978 to 2006 show that lake ice duration is reduced by about 14–15 days. The freeze-up dates are about 4 days later and break-up dates about 10 days earlier. The regression analyses show that, at the 0.05 significance level, the correlations are 0.83, 0.66 and 0.89 between monthly mean air temperature (MMAT) and lake ice duration days, freeze-up dates, break-up dates, respectively. Therefore, inter-annual variations of the Qinghai Lake ice duration days can significantly reflect the regional climate variation.

lake ice, passive microwave remote sensing, freeze-up, break-up, Qinghai Lake, climate change

Many studies have shown that the ice duration on lakes can indicate the regional climate variations, and recently, the remote sensing methods have been proven an efficient way of monitoring the breakup and freeze dates^[1–9]. They can provide an opportunity to get a general idea of the lake ice with repeated periods from the satellites. The visible and near infrared (Vis-NIR) and Synthetic Aperture Radar (SAR) remote sensing data can identify lake ice, and have been used in many successful case studies. However, they lacked the temporal revisit capability necessary to accurately determine the seasonality of the associated processes^[10,11]. Current lower resolution satellite microwave sensors, e.g., NOAA/NASA Pathfinder Program Special Sensor Microwave/Imager (SSM/I), have the potential to resolve the timing of these seasonal transitions on a larger scale. It is well known that there is a large difference in dielectric properties between liquid water and ice, leading to the different

brightness temperatures on the lake during ice and ice-free periods. The high frequency (85 GHz) of the SSM/I had been used to investigate the ice duration of large lakes^[12], but its low frequencies (19 and 37 GHz) are not used for lake ice monitoring. However, the brightness temperature data at high frequencies are easily contaminated by weather conditions, which make their results fluctuate. Furthermore, low frequencies data are available since Nimbus-7 Scanning Multi-channel Microwave Radiometer (SMMR), which can make the records of lake ice duration to the year of 1978.

Therefore, the main objectives of this paper are (1) to test the capabilities of identifying freeze-up and break-

Received October 13, 2008; accepted December, 2008

doi: 10.1007/s11434-009-0044-3

[†]Corresponding author (email: chetao@lzb.ac.cn)

Supported by National Basic Research Program of China (Grand No. 2007CB411506), and National Natural Science Foundation of China (Grand Nos. 40601065 and 40701030)

up dates of lake ice using low frequencies of passive microwave satellites; (2) to conduct a case study on the Qinghai Lake by using the time series of SMMR and SSM/I data; and (3) to analyze the correlations between lake ice duration and monthly mean air temperature (MMAT) from 1978 to 2006.

1 Methodology

The Qinghai Lake is the largest inland lake in China, located in the north-east of Tibet Plateau with an elevation of 3200 m. The surface area of lake is 4500 km², with a mean depth of 25 m. It is a salt water lake, and the average salinity is about 6‰ on a weight basis.

1.1 Microwave dielectric properties of saline water and lake ice

The dielectric constant of the lake water can be estimated by^[13]

$$\varepsilon'_{sw} = \varepsilon_{sw\infty} + \frac{\varepsilon_{sw0} - \varepsilon_{sw\infty}}{1 + (2\pi f \tau_{sw})^2}, \quad (1)$$

$$\varepsilon''_{sw} = \frac{2\pi f \tau_{sw} (\varepsilon_{sw0} - \varepsilon_{sw\infty})}{1 + (2\pi f \tau_{sw})^2} + \frac{\sigma_i}{2\pi \varepsilon_0 f}, \quad (2)$$

where the subscript *sw* refers to saline water, σ_i is the ionic conductivity of the aqueous saline solution in $\Omega^{-1} \text{m}^{-1}$, ε_0 is the permittivity of free space ($\varepsilon_0 = 8.854 \times 10^{12} \text{Fm}^{-1}$) and f is the frequency of microwave radiometer.

Given the $T = 0^\circ\text{C}$, which is the critical temperature of ice and water, the dielectric properties for saline water are calculated. The results show that the real part of saline water is 19.759 for 19 GHz and 9.435 for 37 GHz, while the imaginary part is 31.742 for 19 GHz and 18.824 for 37 GHz, respectively.

For the dielectric properties of lake ice, many researches find that the real part is independent of both temperature and frequency in the microwave region, and can be assigned the constant value (3.15)^[13]. For the imaginary part, we use Nyfors's formula^[14]:

$$\varepsilon''_{ice} = 57.34 \left(f^{-1} + 2.48 \times 10^{-14} \sqrt{f} \right) \exp(3.62 \times 10^{-2} T), \quad (3)$$

where $T = 0^\circ\text{C}$, as well. The results show that the imaginary part is 0.0039 for 19 GHz and 0.0054 for 37 GHz, respectively.

Microwave brightness temperature properties of saline water and lake ice can be obtained by analyzing microwave radiative transfer model for low-infinite space. To ignore the effects of surface roughness and the sky background, the radiometric brightness temperature

(T_B) is given by

$$T_B(f, \theta, p) = e(f, \theta, p)T = [1 - \Gamma(f, \theta, p)]T, \quad (4)$$

the subscripts f , θ , p refer to the frequency, nadir angle, and polarization (h or v), respectively. The e and Γ indicate the emissivity and reflectivity of lake water or ice, and the reflectivity (Γ) as follow:

$$\Gamma(f, \theta, h) = \left| \frac{\cos(\theta) - \sqrt{\varepsilon - \sin^2 \theta}}{\cos(\theta) + \sqrt{\varepsilon - \sin^2 \theta}} \right|^2, \quad (5)$$

$$\Gamma(f, \theta, v) = \left| \frac{\varepsilon \cos(\theta) - \sqrt{\varepsilon - \sin^2 \theta}}{\varepsilon \cos(\theta) + \sqrt{\varepsilon - \sin^2 \theta}} \right|^2, \quad (6)$$

where ε represents the complex dielectric constant of lake water or ice, and h and v stand for horizontal and vertical polarization configurations, respectively.

Given $\theta = 53^\circ$, $T = 0^\circ\text{C}$, the reflectivity and emissivity are calculated. The results are listed in Table 1.

Table 1 Emissivity of saline water and lake ice at 19 and 37 GHz

	Emissivity at 19 GHz		Emissivity at 37 GHz	
	<i>h</i>	<i>v</i>	<i>h</i>	<i>v</i>
Saline water	0.29	0.61	0.36	0.71
Lake ice	0.80	0.99	0.80	0.99

It should be mentioned that the emissivity here is for ideal conditions. (1) The surface roughness is ignored; (2) the lake ice thickness assumed is infinite; and (3) the sky radiation and atmosphere effects are quite small. The ideal conditions can interpolate the essential properties of these two materials in the microwave range. According to eq. (4), and at 0°C physical temperature the brightness temperature of saline water is much smaller than that of lake ice. In other words, the brightness temperature will significantly increase once the lake is frozen, vice versa. It is the basic principle of monitoring the breakup and freeze of the lake.

1.2 Brightness temperature of passive microwave satellite

To avoid the pixel-mixed problem, the brightness temperature data at the centre of Qinghai Lake are selected to illustrate the change between a freeze and breakup period (Figure 1). From summer to the beginning of winter, the physical temperature of lake water decreases which leads to a decline in brightness temperature. In winter, the lake ice occurs around the lake gradually, which causes an increase in brightness temperature due to the higher dielectric constant of ice. In this period, the

pixels of passive microwave remote sensing include the radiative signals from both lake water and ice. After freeze-up, the ice dominates on the lake surface so that the contributions from water can be ignored. Later on the brightness temperature has a small rise as the lake ice thickens. From freeze-up date to break-up date, the brightness temperature is on a sustained high level. When the lake ice breaks up, the contributions from water dominate the brightness temperature again, and the high level disappears. After breakup date, with the warming of lake water temperature, the brightness temperature increases slowly, until next freeze-up/break-up cycle. Therefore, when the brightness temperature data reaches the high level again it means that the lake is frozen.

From Figure 1, the brightness temperature data of lake water fluctuate visibly, due to the surface roughness caused by the wind. On the other hand, the lake ice surface roughness is stable and brightness temperature depends on the lake ice's physical temperature and thickness which change slowly, therefore, brightness temperature data is very steady during the frozen period.

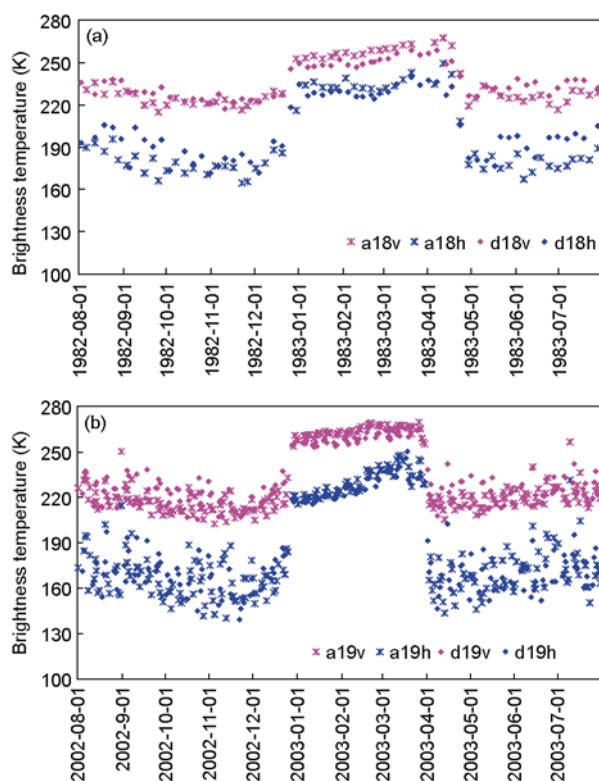


Figure 1 Brightness temperature time series at 18 and 19 GHz for both the horizontal and vertical polarization in a freeze and breakup period (SMMR in 1982/1983 and SSM/I in 2002/2003). Here, a and d indicate the ascending and descending path, while h and v for the horizontal and vertical polarization, respectively.

The freeze-up and break-up dates can be identified by the appearance and disappearance of the high levels. Meanwhile, the fact that this brightness temperature is larger than 200 K (for descending path) or 240 K (for ascending path) is also introduced to eliminate the influence from the fluctuations of brightness temperature of lake water:

$$\text{Min}(\text{Mean}(Tb_i, Tb_{i-1}, Tb_{i-2}) - \text{Mean}(Tb_{i+2}, Tb_{i+1}, Tb_i)) \text{ and } Tb_i > 200 \text{ or } 240, \quad (7)$$

$$\text{Max}(\text{Mean}(Tb_i, Tb_{i-1}, Tb_{i-2}) - \text{Mean}(Tb_{i+2}, Tb_{i+1}, Tb_i)) \text{ and } Tb_i > 200 \text{ or } 240, \quad (8)$$

where i is the Julian day, $\text{Max}()$, $\text{Min}()$ and $\text{Mean}()$ are the maximum, minimum and average values. Tb is the brightness temperature. Formula (7) means that the date of freeze-up is the day when brightness temperature changes from low to high and reaches the high level. On the other hand, formula (8) means that the date of break-up is the day when brightness temperature changes from high to low and leaves the high level.

2 Results and discussions

2.1 Time series of frozen duration of Qinghai Lake

The passive microwave brightness temperature data at low frequency (19 GHz) from 1978 to 2006 were collected to obtain the long-term frozen duration of Qinghai Lake (Figure 2). The SMMR data are come from 1978

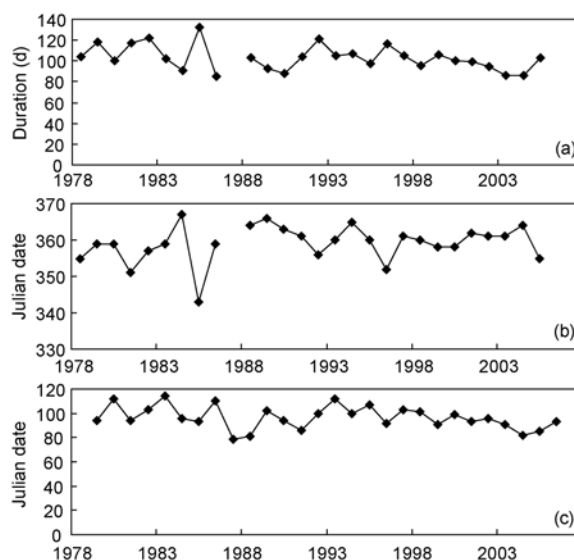


Figure 2 Time series of frozen duration dates of Qinghai Lake based on the passive microwave brightness temperature data from 1978 to 2006. (a) Duration dates from 1979 to 2005, (b) freeze-up dates from 1978 to 2005, (c) break-up dates from 1979 to 2006. Note: here the Y-axis presents the Julian date, and when the date value is larger than 365 it means the freeze-up occurred in the next year.

to 1987, while the SSM/I data from 1987 to 2006. When the lake center froze-up or broke-up, the date was recorded as the beginning or end of frozen period. Unfortunately, there are no data from December 3, 1987 to January 12, 1988, so there is no record of this freeze-up day.

The Qinghai Lake is located at a middle latitude zone (even a little low latitude), and there is a gap between satellite passes. For the SSM/I data, there are two or three days of continuous gaps after four or five days of observations. Fortunately, the ascending and descending orbits have a two days offset so that the continuity can be improved to one or two days gaps. With the SMMR data, the problem of gaps is larger due to the sample period of every two days. When both of ascending and descending orbits data are used, the gaps can be improved to two or four days. In the worst case, the time series of frozen duration of Qinghai Lake has a temporal resolution of two or four days (1978 to 1987) and one or two days (1987 to 2006). The data from 1978 to 2006 show that lake ice duration dates are reduced by about 14–15 days, while freeze-up dates are later by about 4 days and break-up dates be earlier by about 10 days.

2.2 Validation

For the measurement of the lake ice data, the Qinghai Lake hydrological station was used, which is about 1 km from the South bank. The lake ice data from 2002 to 2006 include the freeze-up and break-up dates, as well as the lake ice thickness. Here, the freeze-up and break-up dates in recent years are used to compare with the results from the passive microwave remote sensing data (Table 2). The estimations using passive microwave remote sensing data agree well with the measurements *in-situ*, except that the freeze-up dates in 2002 and 2005 and the break-up date in 2002 have differences of two days. Checking the raw brightness temperature data from satellite, it was found that the revisit frequency is

Table 2 Comparison of freeze-up and break-up dates between the measurements *in situ* and the estimation from passive microwave remote sensing data

Freeze-up date		Break-up date	
Observation <i>in situ</i>	SSM/I data	Observation <i>in situ</i>	SSM/I data
2002-12-26	2002-12-28	2002-04-06	2002-04-08
2003-12-27	2003-12-27	2003-03-31	2003-04-01
2004-12-30	2004-12-30	2004-03-20	2004-03-20
2005-12-19	2005-12-21	2005-03-26	2005-03-26
2006-12-23	2006-12-24	2006-04-04	2006-04-03

the main reason. In the Qinghai Lake area, there is no data on April 6 and 7, 2002, and there is no data on December 19 and 20, 2005.

The station measurements can only show the point information. For the areal validation of the results, the MODIS L1B reflectance data in the freeze and breakup transitional period of 2002 and 2003 were collected. The MODIS L1B data were obtained from the Goddard Earth Sciences Distributed Active Archive Center (GES DAAC) at <http://daac.gsfc.nasa.gov/>. The composite images of MODIS reflection data from band 6, 2, and 1 can clearly distinguish between water and ice (Figures 3 and 4).

In the freeze-up period (Figure 3), MODIS images show that lake ice dominates the lake surface on December 27. The SSM/I data show the frozen date is on December 28. In the break-up period (Figure 4), MODIS images show that water dominates the lake surface on April 1, the SSM/I data show the same day.

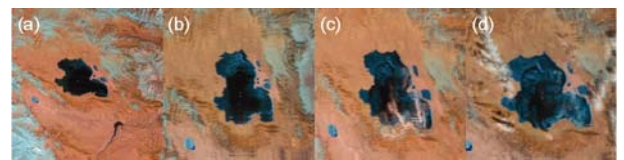


Figure 3 Composite images of MODIS reflection data from band 6, 2, and 1 which show the freeze-up process from December 24 to 27, 2002.

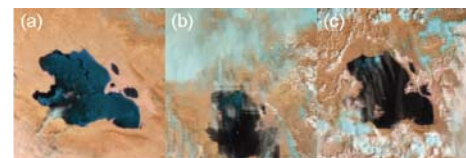


Figure 4 Composite images of MODIS reflection data from band 6, 2, and 1 which show the break-up process on March 30, April 1 and 3, 2003. The cloud covered the lake on March 31 and April 2.

2.3 Relationship between frozen duration and air temperature

The MMAT data from 1978 to 2005 at the Gangcha meteorological station to Qinghai Lake are statistically compared with the frozen duration of Qinghai Lake (Table 3). Under the 0.05 significant level, the correlation is 0.83 (Figure 5). Furthermore, the lake ice duration dates include the information of both the freeze-up date and break-up date, these two dates were also compared (Figures 6 and 7). The correlations between the lake ice freeze-up dates and MMAT is 0.66, while that of the break-up dates is 0.89. The current results show that the

Table 3 Results of regression analysis between lake ice duration, freeze-up dates and break-up dates and monthly mean air temperature (MMAT) from 1978 to 2005

Statistics	Duration	Freeze-up date	Break-up date
Regression coefficient R	0.83	0.66	0.88
Regression coefficient R_{sqr}	0.69	0.43	0.77
Intercept	-53.25	398.94	-40.26
Slope of MMAT in January	-4.92	0.68	-2.04
Slope of MMAT in February	-3.91	-0.30	-3.31
Slope of MMAT in March	-0.13	-3.03	-1.60
Slope of MMAT in April	-0.81	1.44	-1.85
Slope of MMAT in May	-1.71	-0.06	-0.68
Slope of MMAT in June	1.34	0.35	2.35
Slope of MMAT in July	1.59	2.04	2.50
Slope of MMAT in August	-0.09	0.65	-0.27
Slope of MMAT in September	2.85	-1.08	0.03
Slope of MMAT in October	-2.34	-0.08	0.13
Slope of MMAT in November	-3.24	0.84	-2.97
Slope of MMAT in December	-2.45	0.18	-2.67

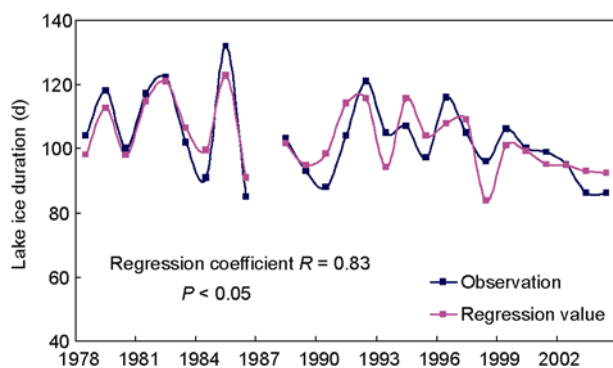


Figure 5 Results of the regression analysis between lake ice duration and monthly mean air temperature data from 1978 to 2005.

variation of lake ice duration records obviously depend on the regional air temperature changes. The lake ice break-up date is more sensitive to the regional increased air temperature. The low correlation between freeze-up dates and MMAT may be due to other climate conditions, such as precipitation and wind.

3 Conclusions

The freeze-up and break-up dates are monitored using satellite passive microwave remote sensing low frequency data. The validation by the hydrological station

- 1 Palecki M A, Barry R G. Freeze up and break up of lakes as an index of temperature changes during the transition seasons: A case study for Finland. *J Appl Meteor*, 1986, 25: 893–902
- 2 Schindler D W, Beaty K G, Fee E J, et al. Effects of climatic warming

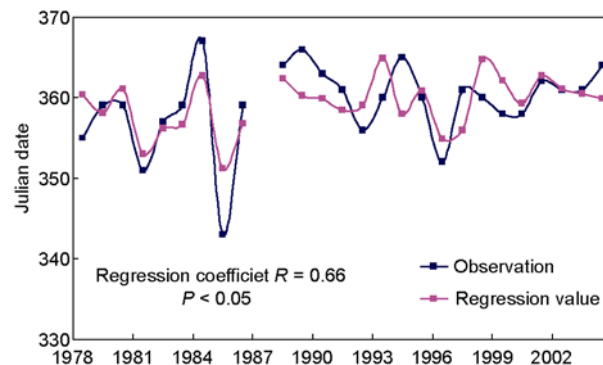


Figure 6 Results of the regression analysis between freeze-up dates and monthly mean air temperature data from 1978 to 2005.

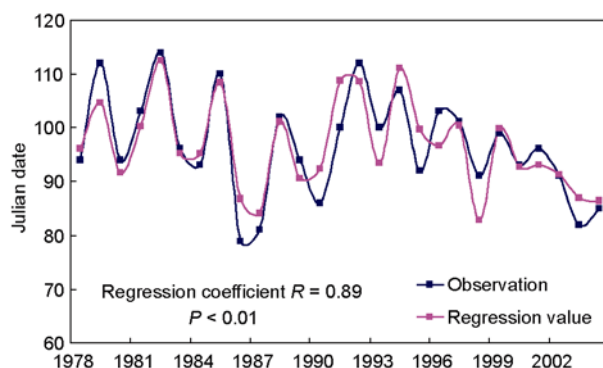


Figure 7 Results of the regression analysis between break-up dates and monthly mean air temperature data from 1978 to 2005.

and the MODIS data proved that this method is accurate. The results monitored from 1978 to 2006 show that the lake ice duration is reduced by about 14 to 15 days. Furthermore, the freeze-up dates are about 4 days later and break-up dates about 10 days earlier. The correlation between lake frozen duration and MMAT is very significant, and the break-up date is more sensitive to the regional air temperature variation.

The influence of weather conditions on microwave remote sensing low frequency can be ignored, therefore, the time series of passive microwave remote sensing data can easily used to analyze the frozen duration of global large lakes.

The authors wish to sincerely thank two anonymous reviewers whose comments greatly improved the quality of the paper. The remote sensing data were obtained from the National Snow and Ice Data Center, and the lake ice duration data from the Qinghai Lake hydrological station.

- on lakes of the central boreal forest. *Science*, 1990, 250: 967–970
- 3 Robertson D M, Ragotzkie R A, Magnuson J J. Lake ice records used to detect historical and future climatic changes. *Clim Change*, 1992, 21: 407–427

- 4 Walsh S E, Vavrus S J, Foley J A, et al. Global patterns of lake ice phenology and climate: Model simulations and observations. *J Geophys Res*, 1998, 103: 28825–28837
- 5 Magnuson J J, Roberston D M, Benson B J, et al. Historical trends in lake and river ice cover in the Northern Hemisphere. *Science*, 2000, 289: 1743–1746
- 6 Duguay C R, Pultz T J, Lafleur P M, et al. RADARSAT backscatter characteristics of ice growing on shallow sub-Arctic lakes, Churchill, Manitoba, Canada. *Hydrol Proc*, 2002, 16: 1631–1644
- 7 Todd M C, Mackay A W. Large scale climatic controls on Lake Baikal ice cover. *J Clim*, 2003, 16: 3186–3199
- 8 Weyhenmeyer G A, Meili M, Livingstone D M. Nonlinear temperature response of lake ice breakup. *Geophys Res Lett*, 31: L07203, doi:10.1029/2004GL019530
- 9 Johnson S L, Stefan H G. Indicators of climate warming in Minnesota: Lake ICE covers and snowmelt runoff. *Clim Change*, 2006, 75: 421–453
- 10 Hall D K, Riggs G A, Salomonson V V, et al. MODIS snow-cover products. *Remote Sens Environ*, 2002, 83: 181–194
- 11 Pietroniro A, Leconte R. A review of Canadian remote sensing and hydrology, 1999–2003. *Hydrol Proc*, 2005, 19: 285–301
- 12 Walker A E, Davey M R. Observation of Great Slave Lake ice freeze-up and break-up processes using passive microwave satellite data. In: *Proceedings of the 16th Canadian Remote Sensing Symposium*, Sherbrooke, Quebec, Canada, 1993. 233–238
- 13 Ulaby F T, Moore R K, Fung A K. *Microwave Remote Sensing: Active and Passive. Volume III: from Theory to Applications*. Norwood, MA: Artech House, 1986. 1065–2162
- 14 Kendra J R, Sarabandi K, Ulaby F T. Radar measurements of snow: experiment and analysis, *IEEE Trans Geosci Remote Sens*, 1998, 36: 864–879